Time-Resolved Study of the Inner Space of Lactose Permease

E. Nachliel,* N. Pollak,* D. Huppert,† and M. Gutman*

*Department of Biochemistry, Laser Laboratory for Fast Reactions in Biology, George Wise Faculty of Life Science, Tel Aviv University, Tel Aviv 69978, Israel, and †School of Chemistry, Raymond and Beverly Sackler Faculty of Exact Sciences, Tel Aviv University, Tel Aviv, Israel

ABSTRACT Pyranine (8-hydroxy pyrene-1,3,6-trisulfonate) is a commonly used photoacid that discharges a proton when excited to its first electronic singlet state. Follow-up of its dissociation kinetics reveals the physicochemical properties of its most immediate environment. At vanishing ionic strength the dye adsorbs to the *Escherichia coli* lactose permease with stoichiometry of 1:1 and an association constant of $2.5 \times 10^5\ M^{-1}$. The reversal of the binding at high ionic strength and the lower pK value of the bound dye imply that positive charge(s) stabilize the dye in its site. The fluorescence decay curve of the bound dye was measured by time-correlated single photon counting and the measured transient was subjected to kinetic analysis based on the geminate recombination model. The analysis indicated that the binding domain is a cleft (between 9 and 17 Å deep) characterized by low activity of water ($a_{(water)} = 0.71$), reduced diffusivity of protons, and enhanced electrostatic potential. The binding of pyranine and a substrate are not mutually exclusive; however, when the substrate is added, the dye-binding environment is better solvated. These properties, if attributed to the substrate-conducting pathway, may explain some of the forces operating on the substrate in the cavity. The reduced activities of the water strips the substrate from some of its solvation water molecules and replace them by direct interaction with the protein. In parallel, the lower dielectric constant enhances the binding of the proton to the protein, thus keeping a tight seal that prevents protons from diffusing.

INTRODUCTION

The lactose permease (lac permease) of *Escherichia coli* catalyzes the coupled translocation of β galactosides and H^+, in a stoichiometry of 1:1, across the cytoplasmic membrane of the bacterium (reviewed in Viitanen et al., 1986; Kaback and Wu, 1997). The enzyme is composed of a bundle of loosely packed, rigid transmembranal helices with a few residues that are essential for the mechanism. Site-directed structural approaches and extensive mutational analysis have led to a proposed helix packing model for lac permease (Kaback et al., 1997; Frillingos et al., 1998; Kaback, 1997)

The transported substrate is an uncharged hydrophilic molecule that is driven by vectorial binding and dissociation of a proton. Thus, there must be a mechanism that couples the reversible charging of the protein with a replacement of the hydration shell of the free substrate by protein-substrate interaction. In the present study we looked for evidence for modulation of the hydration of the protein during its interaction with its substrate. The detection of the hydration level is based on time-resolved fluorescence measurements of an excited pyranine molecule (8-hydroxy pyrene-1,3,6-trisulfonate, ϕOH). In its excited state, the redistribution of the π orbital electrons lowers the pK of the hydroxy moiety from $pK_0 = 8.2$ to $pK^* = 1.4$ and the proton dissociates with a time constant of 100 ps. This rate of dissociation is very sensitive to the capacity of the immediate vicinity to solvate the proton within a timeframe comparable to the stretching frequency of the OH bond (Huppert et al., 1982). Thus, monitoring the fluorescence of the pyranine molecule can reflect a local variation of the activity of the water within the most immediate vicinity of the dye. The pyranine molecule has three negative charges and an extended π orbital surface that can participate in hydrophobic interactions with the protein. The combination of these two forces enables it to adsorb both to neutral phospholipid membranes (Clement and Gould, 1981; Rochel et al., 1990), or to charged domains on a protein (Yam et al., 1991). In the present study we noticed that, at low ionic strength, the pyranine forms a 1:1 tight complex ($\Delta G \sim -7.5$ Kcal/mol) with the protein, which is stabilized by electrostatic interactions.

The observed parameter in this study is the well-documented property of pyranine to gain thermodynamic stability in its excited state by dissociating to an ion pair ($\phi O^{*-} + H^+$) (Forster and Volkers, 1975; Weller, 1961). The dynamics of dissociation are detected by picosecond fluorescence measurements (Rochel et al., 1990; Gutman and Nachliel, 1993), and analyzed by the geminate recombination model of Agmon (Agmon and Szabo, 1990; Krissinel and Agmon, 1996). The analysis is based on numerical reconstruction of the translational diffusion of a proton within the electrostatic field of the excited anion, according to the Debye-Smoluchowski time-dependent diffusion equation. The analysis incorporates the contribution of the shape of the diffusion space, the effective dielectric constant, and the diffusion coefficient of the proton into a set of transition probabilities along a diffusion trajectory. The propagation of the proton in time and space, according to

Received for publication 24 March 2000 and in final form 6 December 2000.

Address reprint requests to Dr. M. Gutman, Department of Biochemistry, Laser Laboratory for Fast Reactions in Biology, George Wise Faculty of Life Science, Tel Aviv University, Ramat Aviv 69978, Israel. Tel.: 972 -3 -640 -9875; Fax: 972 -3 -640 -6834; E-mail: me@hemi.tau.ac.il.

0006-3495/01/03/1498/09 $2.00

the transition probabilities, reconstructs the observed fluorescence decay dynamics (Pines et al., 1988). By this method, we had investigated the physical properties of a microscopic space at the heme binding site of apomyoglobin (Gutman and Nachliel, 1993), the anion-specific channel of PhoE of *E. coli* (Gutman et al., 1992), and the intermembranal space in multilamellar phospholipid vesicles (Rochel et al., 1990).

The analysis of the fluorescence decay dynamics of the pyranine when bound to lac permease revealed that it is located in a rather deep cleft, where the water molecules strongly interact with the protein. The binding site appears to be coupled with the substrate binding site but is not identical with it; the substrate or its analog modulates the fluorescence properties of the dye without displacing it from its binding site. We regard this observation as evidence that the insertion of the substrate alters the structure of the protein in a mode that affects the physical properties of its solvation water.

MATERIALS AND METHODS

Purified lac permease was a generous gift from R. Kaback and J. Le Coutre, (Howard Hughes Medical Institute, UCLA, Los Angeles, CA). Pyranine (8-hydroxy pyrene-1,2,6-trisulfonate (Na^+ salt), laser grade) was purchased from Sigma, St. Louis, MO.

Binding of pyranine to lac permease

The protein was dissolved in 0.018% LM (*n*-dodecyl-β-D-maltoside) to a final concentration of 5.7 μM and the pyranine was added to the desired concentration. To maintain a constant pH and low ionic strength, the solution was buffered by low concentration (50 μM) of Hepes buffer (pH 6.8) in the absence of other salt.

Steady state fluorimetry was measured with a Shimadzu RF540 spectrofluorimeter. Time-resolved fluorescence was measured with a 200 μl solution of the dye-protein complex. The instrumental setup for the time-resolved fluorescence consisted of a mode-locked Nd-Yag laser, pumping a cavity damped dye laser followed by frequency doubling (300 nm). The fluorescence of the protonated excited pyranine, ϕOH*, was monitored by a time-correlated single photon counting system (for more experimental details see Pines et al., 1988).

Mathematical model of analysis

The analysis of the fluorescence decay of ϕOH* emission was carried out by the program of Agmon that reconstructs the experimental signal trough numerical integration of the differential form of the Debye-Smoluchowski equation for diffusion-controlled reaction (Agmon and Szabo, 1990; Krissinel and Agmon, 1996; Pines et al., 1988; Huppert et al., 1990; Agmon et al., 1988). The reconstruction of the proton propagation, after the excitation, incorporates two parallel processes: 1) the reversible dissociation at the surface of the reaction sphere (r_0). The process is quantified by two rate constants: the dissociation (κ_f) and recombination of the proton with the excited pyranine anion (κ_r). 2) The dispersion of the proton in the reaction space. This process is operative in the space defined by $r > r_o$ and is modulated by three parameters: i) the intensity of the electrostatic potential that attracts the proton to the pyranine anion that is quantitated by the Coulomb cage radius (R_D); ii) the entropic term that favors the dispersion of the proton. This term reflects the geometry of the dispersion space; and iii) the diffusion coefficient of the proton that regulates how fast the proton will probe the reaction space.

The analysis of the observed signal combines all these terms into a set of transition probabilities that define the probability that a proton in a concentric shell (*i*) will progress to the next one (*j*) as given by Eq. 1:

$$TP_{ij} = D_{H+}/\Delta r^2 \cdot f^{(n)}(r_i/r_j) \cdot \exp[-R_D/2 \cdot (1/r_i - 1/r_j)] \quad (1)$$

The first term in Eq. 1 is the diffusion coefficient (D_{H+}) of the proton and the width of the shells (Δr = 1 Å). This term sets the basic frequency of the transition between the shells and its value is $\sim$3–9 $\times$ 10^{11} s^{-1}, depending on the diffusion coefficient. The second term ($f^{(n)}(r_i/r_j)$) represents the preference of the proton to diffuse from shell (*i*) to shell (*j*) that differ in the number of equipotential sites where *n* is the dimensionality of the diffusion space. For $n = 3$ the value of $f^{(3)}(r_i/r_j)$ is equal to r_i/r_j, while for a one-dimensional space, $f^{(1)}(r_i/r_j) \equiv 1$. The last term in Eq. 1 denotes the gradient of the electrostatic pair potential. The Debye radius, R_D, (see Eq. 2) is the distance at which the dielectric constant of the diffusion medium reduces the electrostatic potential to the level of thermal energy and its magnitude varies with the effective dielectric constant of the environment.

$$R_D = Z_1 Z_2 e_0^2/\varepsilon_{eff} k_B T \quad (2)$$

The program combines the chemical reaction at the surface of the excited molecule, r_0, defined as the rate of proton ejection (κ_f in s^{-1}) and recombination rate (κ_r in Å s^{-1}), with the diffusion process described by the transition probabilities given in Eq. 1. It propagates the perturbation in time and space, calculating the probability density of the proton by the Chebyshev expansion method (Agmon and Szabo, 1990).

In the present case the diffusion space is approximated as a well having a radius of r_w ($r_w \geq r_0$) and a depth of r_d (Shimoni et al., 1993; Gutman et al., 1992) In the present reconstruction we considered a proton that reaches the end of the channel to be irreversibly lost to the bulk.

The program in a simple PC version has been published (Krissinel and Agmon, 1996) and is available upon request from Prof. Noam Agmon, the Fritz-Haber Institute, Hebrew University of Jerusalem, Israel.

RESULTS AND DISCUSSION

Binding of pyranine to the lac permease

The pyranine molecule can be excited at two wavelengths: at 450 nm only the ionized form ϕO^- is excited and the measured emission is at 515 nm. Excitation at 400 nm excites the ϕOH state and the measured emission appears as a main band at 515 nm with a shallow shoulder at $\sim$440 nm. The reason for the enhanced emission of ϕO^{*-}, even when ϕOH is the excited species, is the rapid dissociation of ϕOH* at a rate that exceeds the decay to the ground state (Yam et al., 1991; Forster and Volkers, 1975). The fluorescence lifetimes of the two forms (ϕOH*, ϕO^{*-}) are almost the same, 5.0 and 4.8 ns respectively, and are not affected by the solvent. Accordingly, the enhanced emission of ϕO^{*-}, even when the excited species is ϕOH, implies that in water most of the excited dye molecules discharged their proton before decaying to the ground state.

The emission spectrum of pyranine in the presence of lac permease or in LM is shown in Fig. 1. The spectrum as measured either in pure water or in the presence of the detergent, is identical in shape, and the intensity of the emission of the ϕOH* is 5% $\pm$ 0.05% with respect to that

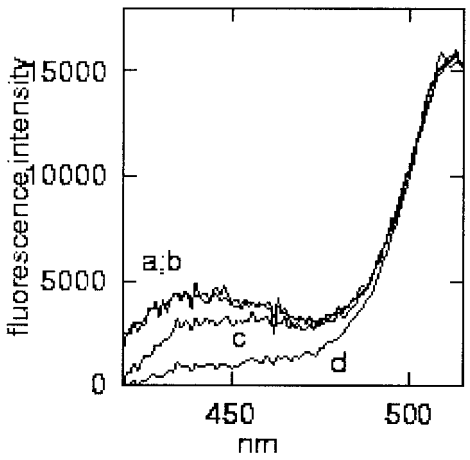

FIGURE 1 Fluorescence emission spectra of the pyranine-lac permease complex. The emission spectra were measured with excitation at $\lambda = 350$ nm with a solution containing 5 μM lac permease, 0.018% LM, 100 μM Hepes buffer, pH = 6.5. *Traces a* and *b* were recorded in the presence of 80 nM pyranine or 80 nM pyranine plus 20 mM sucrose. *Trace c* was recorded after addition of 20 mM TDG. *Trace d* was measured after addition of NaCl to final concentration of 50 mM and is identical with the spectrum recorded with 80 nM pyranine in LM.

of the ϕO^{*-} (data not shown). This ratio implies that there is no adsorption of the dye to the detergent micelles. In the presence of the enzyme the emission at ~440 nm was significantly intensified, up to 27% of the intensity measured at 515 nm (Fig. 1, *curve a*). The enhanced emission of the ϕOH* implies that the dye is in a new environment, one that slows the dissociation with respect to the fluorescence lifetime of the dye. Addition of sucrose had no effect on the emission spectrum (*curve b*), but addition of 20 mM β,galactopyranosyl 1-thio-β,galactopyranoside (TDG) lowered the ratio to 19% (*curve c*). Considering the high affinity of TDG to the enzyme, the marginal reduction of the ratio implies that TDG did not displace the dye from its binding site, but rather modified the physicochemical properties of the dye's binding site. Thus, the site we are probing by the pyranine molecule is not that to which the substrate is bound, but is close enough to detect the conformational changes caused by its binding. The selective deformation of the dye's emission by a substrate analog, and not by a molecule of comparable mass and solvation properties, implies that the binding site is within the protein itself and is not some traces of co-purified lipids that were carried into the micelle. At high ionic strength (100 mM NaCl) the dye dissociates and the intensity of the emission at 435 nm (*curve d*) is identical to that measured for the free dye.

The binding of pyranine to the lac permease was measured by a fluorescence titration, monitoring the ratio of the two emission bands as a function of the dye/protein ratio, and analysis of the results according to Gutman and coworkers (Shimoni et al., 1993; Gutman et al., 1982). For each sample the fraction of the bound ligand was calculated and the data were drawn according to a Scatchard plot. The intercepts yielded an association constant of the dye $K = 2.5 \pm 0.7 \times 10^5\ M^{-1}$ and a dye/protein stoichiometry of 1:1. This ratio is also indicative that the dye is bound to the enzyme and not to phospholipids that was carried over with the protein.

The pK of the pyranine in the complex was calculated from the ratio of the excitation bands of the two ground state species (400 nm for ϕOH and 460 nm for ϕO^-). The titration was carried out with 5.7 μM lac permease in the presence of 300 nM pyranine, conditions where ~42% of the pyranine was free. The apparent pK value of the bound dye, where half of it was in the protonated state, was 7.4 ± 0.05. This value is significantly lower than pK = 8.2 that is measured in water at vanishing ionic strength (Pines et al., 1988). However, as we could not exclude the possibility that the titration curve was distorted by the emission of some free dye, the actual pK of the bound pyranine could be even lower.

The low pK value of the bound pyranine and the reversal of binding at high ionic strength indicate that the binding is attained through electrostatic interaction of the dye with one or more positive charges in the protein. The steady-state fluorescence measurements clearly indicate that the environment in which the pyranine is bound differs from bulk water, yet it provides no information on its nature and which mechanism leads to the diminished emission of ϕOH in the presence of the substrate. For this reason, the time-resolved fluorescence was investigated.

Time-correlated single photon counting

Kinetics measurements of the fluorescence decay of excited pyranine bound to the lac permease were carried out, and the results are shown in Fig. 2 *A*. The fastest relaxing curve (*line a*) was measured for the dye (300 nM) in the presence of 0.018% LM. The relaxation commences with a fast decay corresponding to the dissociation of the excited molecule, followed by a slow, shallow "tail" where the recombination between the proton and the excited anion regenerates some of the ϕOH*. This kinetic is identical with those measured in pure water (not shown). In the presence of 5.7 μM lac permease (*line b*), the dye is partially bound to the protein and its relaxation dynamics has new features. The most initial rate of the relaxation (first 100 ps) is significantly slower (see inset for the expansion of the first 3 ns), and the tail is more prominent. Addition of substrate (14.3 mM lactose, *line c*) accelerated the decay, but not to the level measured in the absence of the protein. Thus, either some of the pyranine was released from the protein or the substrate (lactose) modulated the physicochemical features of the dye's environment. This effect was specific to the protein dye complex, as comparable concentrations of lactose

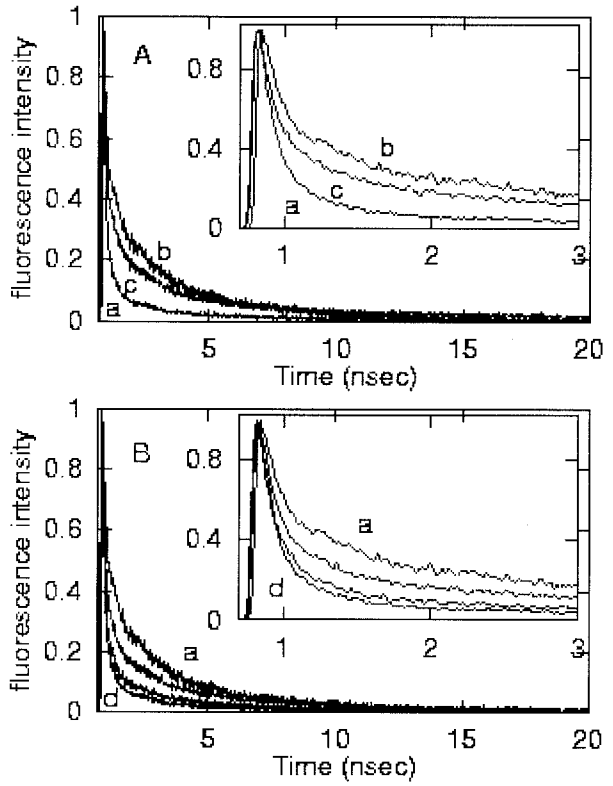

FIGURE 2 (*A*) Fluorescence decay curves of pyranine complexed with lac permease. The measurements were carried out in 0.018% detergent, 5.7 μM enzyme, and 14.3 mM lactose (as indicated) at pH = 6.8. Excitation wavelength 300 nm; emission 435 nm. Total observation time 20 ns. The ordinate is the fluorescence intensity normalized with respect to the maximal measured value. *Trace a* is a control curve and corresponds with pyranine dissolved in lauryl maltoside and in the absence of enzyme; *trace b* was measured for the pyranine lac permease complex stabilized in lauryl maltoside; *trace c* was measured for the sample defined in *b* after addition of 14.3 mM lactose. The inset expands the transient during the first 3 ns. (*B*) Titration of lac permease by increasing concentrations of pyranine. Fluorescence decay curves measured as in (*A*) with increasing pyranine concentrations. The top curve (*a*) was measured with 300 nm pyranine. The bottom curve (*d*) was measured in the absence of lac permease and corresponds with the signal of the free dye. The other two curves from top to bottom were measured with 600 and 1500 nM pyranine, respectively. The inset expands the dynamics during the first 3 ns.

added to the dye in water or in LM solution had no effect on the relaxation dynamics (not shown).

Fig. 2 *B* depicts the fluorescence decay curves as measured in the presence of increasing dye concentrations. For comparative purposes all signals were normalized to maximal amplitude. At low dye concentration (300 nm, *curve a*) the fraction of the bound dye is maximal and the measured decay is indeed the slowest of the whole series of measurements. At increasing pyranine concentrations the fraction of the free dye increases and the measured dynamics gradually assume the features of the free dye. At pyranine concentrations of 2.0 μM and above the signals are undistinguishable from those measured for pyranine in a LM solution (*curve d*).

Kinetic analysis

The analysis of the measured signals was carried out by the algorithm of Agmon (Gutman and Nachliel, 1993; Agmon and Szabo, 1990; Krissinel and Agmon, 1996; Pines et al., 1988; Shimoni et al., 1993; Gutman et al., 1992a,b) and the results are shown in Fig. 3 where the analysis was carried out for the control signal as measured in 0.018% LM. The main frame depicts the observed dynamics and its reconstructed curve on a linear scale. The inset depicts the same data on a logarithmic scale, emphasizing the accuracy of the fit at the longer time scale, where the signal had decayed to 1% of its initial size. The deviation of the reconstructed curve from the experimental one is presented in the bottom part of the main frame, where for the sake of clarity the baseline was shifted to -0.1. The kinetic parameters characterizing the reactions at the solvation shell of the dye (κ_f and κ_r), the dielectric constant of the reaction space and diffusion coefficient of the proton, were identical to those determined for the reaction in pure water (Table 1, column 2).

The first step in the analysis of the dye-protein complex was to eliminate the contribution of the free dye. Using the measured dissociation constant and the reactant concentrations, the fraction of the free dye equilibrated with 5.7 μM protein at 300 nM and 600 nM pyranine was calculated to be $\alpha_{\phi OH\ free} = 42\%$ and 46%, respectively. To correct for the contribution of the free dye to the measured signal, the normalized fluorescence decay curve measured with the dye-lac permease complex was adjusted by subtracting the appropriate fraction $\alpha_{\phi OH\ free}$ of the free dye signal from the measured signal. The adjusted signals were subjected to kinetic analysis, and experimental curves together with the reconstructed dynamics are shown in Fig. 4. The adjusted

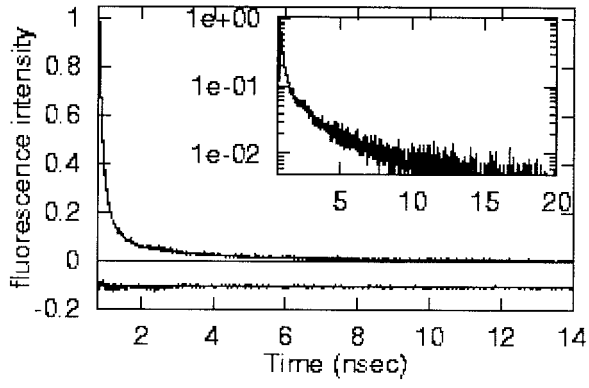

FIGURE 3 Reconstruction of the fluorescence decay curve of pyranine in 0.018% LM. The signal is the one presented in Fig. 2 *A*, *curve a*. The ordinate is the fluorescence intensity normalized with respect to the maximal measured value. The reconstructed curve is superpositioned over the experimental one. The curves are presented on a linear scale (*main frame*) logarithmic one (*inset*). The bottom section of the main frame shows the difference between the reconstructed signal and the experimental one. For the sake of clarity it was shifted to $y = -0.1$. The parameters reconstructing the experimental curve are listed in Table 1.

TABLE 1 The characteristic parameters of the pyranine binding environment in lac permease

Parameter	Pyranine in lauryl maltoside	Pyranine in lac permease	Pyranine in lac permease + lactose
κ_f	7.2×10^9/s	0.65×10^9/s	0.8×10^9/s
κ_r	7.0×10^9 Å s^{-1}	0.75×10^9 Å s^{-1}	0.8×10^9 Å s^{-1}
$a_{(water)}$	1.00	0.71	0.73
D_{H^+}	9.3×10^{-5} cm^2/s*	3×10^{-5} cm^2/s	3×10^{-5} cm^2/s
R_D	28.3 Å†	50. Å	42.5 Å

*The diffusion coefficient of proton in bulk water.
†The Coulomb cage radius of pyranine in water is the theoretical value calculated for a charge of $Z = -4$ at 25°C.

signals as measured with 300 and 600 nM pyranine (*A* and *B*, respectively) are practically identical and were simulated with the same set of parameters. The adjusted signal of the experiment carried out with 1.5 μM dye was similar to the previous two signals, but was too noisy for precise kinetic analysis. The parameters determined for the complexed dye are given in Table 1, column 3.

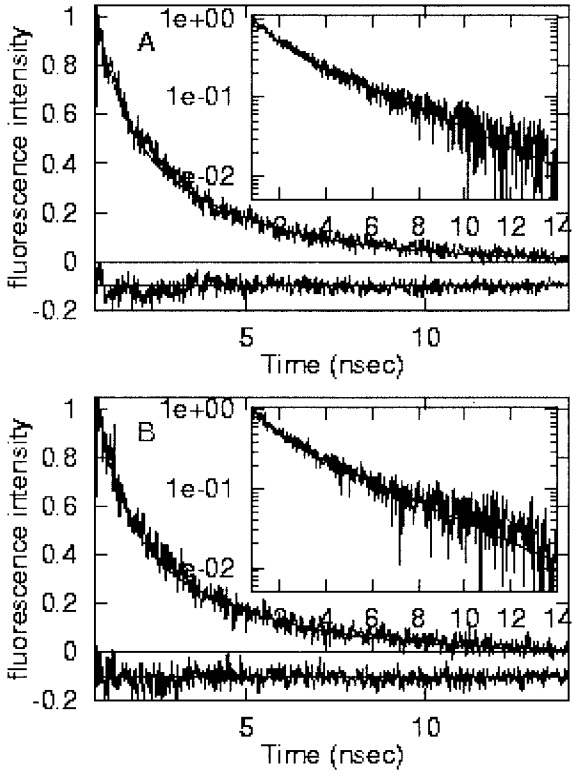

FIGURE 4 Kinetic analysis of the fluorescence decay curves of pyranine adsorbed to lac permease. (*A*) and (*B*) correspond with the transients of the signals measured with 300 nM and 600 nM, respectively, after subtraction of the contribution of the free dye. The ordinate is the fluorescence intensity normalized with respect to the maximal measured value. The main frame depicts the reconstruction on a linear scale while the insets present the dynamics on a logarithmic scale to emphasize the quality of the fit on a longer time scale. The bottom section of the main frame shows that the fit has no systematic deviation from the experimental data. The fractions of bound dye for *A* and *B* are 58% and 54%, respectively. The measurements were carried out with 5.7 μM lac permease in 0.018% LM at pH 6.8.

The effect of lactose on the pyranine decay dynamics

Lactose in the range of 10–100 mM has no effect on the fluorescence decay of pyranine, either when measured in water or in LM solution. This is in accord with our previous observation that sugars affect the decay dynamics of pyranine only at concentrations exceeding 1 M (Gutman et al., 1992a). Addition of a substrate, either TDG or galactose, affected the steady state and the fluorescence decay emission of the bound pyranine (see Figs. 1 and 2). The modulation of the emission can be attributed either to displacement of some of the dye by the substrate, or to the altered environment of the bound dye caused by the binding of the substrate to another site on the protein.

To find out whether the lactose displaced the pyranine, we tried to subtract increasing fractions of the free dye signal from that measured in the presence of lactose. In the absence of lactose, the ratio (bound/free of the pyranine), calculated on the basis of the dissociation constant, was 0.58/0.42. When lactose displaces some of the pyranine from the site, a lower ratio is expected. Accordingly, we subtracted an increasing fraction of the free-dye signal from the signal measured with 14.3 mM lactose. This procedure caused an unacceptable distortion of the signal. The pyranine fluorescence rise time is the sum of the laser pulse width plus the instrumental response time, and is $\tau = 45$ ps with the present setup. Yet, as seen in *A*, increasing the free dye fraction by as little as 4% distorted the shape of the curve by introducing an artificial rise time that is much longer than the instrumental one. A careful adjustment of the $\alpha_{\phi OH\ free}$ value for the signal measured in the presence of lactose was carried out, in a search for a subtracted signal with no artificial rise time. The search yielded the curve shown in *B*, where the ratio of bound/free equals (0.59/0.41), which is essentially identical to that determined in the absence of the substrate. We conclude that the lactose did not displace the dye from the protein, but rather altered the immediate environment of the pyranine. This observation is in accord with the proposed conformation changes caused by binding of substrate (Wu et al., 1995; Pazdernik et al., 1997; Jessen-Marshall et al., 1997). The reconstruction of the fluorescence decay measured in the presence of lactose is presented in Fig. 5 *A*, and necessitated alteration of some of the parameters. These values are given in Table 1, column 4.

Evaluation of the accuracy of the simulating parameters

Before we evaluate the magnitudes of the parameters that characterize the reaction space, it is necessary to establish

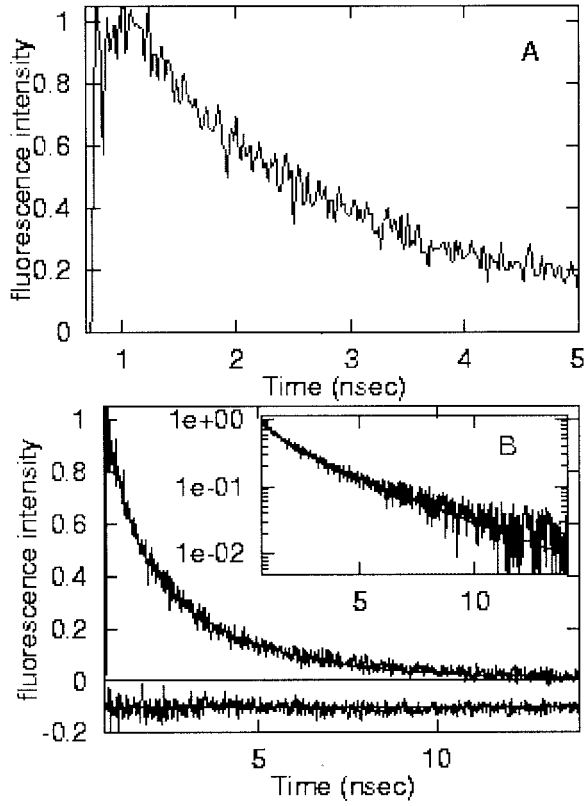

FIGURE 5 Fluorescence decay dynamics of pyranine adsorbed to lac permease in the presence of saturating concentration of lactose. The ordinate is the fluorescence intensity normalized with respect to the maximal measured value. (*A*) Depiction of the distortion of the shape of the kinetic when the fraction of free dye was increased to 45%. Please note the appearance of an artificial rise time followed by a delay in the appearance of the decay. (*B*) Kinetic analysis of the signal measured with 14.3 mM lactose corrected for 41% free dye. The kinetic parameters are listed in Table 1. The inset depicts the same reconstruction on a logarithmic scale and the absence of systematic deviation is presented in the bottom section of the main frame.

the accuracy of these magnitudes. Five parameters are needed to reconstruct the measured dynamics: κ_f, κ_r, R_D, D_{H+}, and r_d.

The parameters κ_f, κ_r are the respective rate constants at which the excited dye ejects or recombines with a proton at the surface of its reaction sphere (r_0 = 6 Å) (Pines et al., 1988). R_D is the effective Debye radius of the pyranine anion and reflects the charge of the dye and the dielectric constant of the environment (see Eq. 2 above). D_{H+} is the diffusion coefficient of the proton (in water $D_{H+} = 9.3 \times 10^{-5}$ cm^2 s^{-1}). Finally, the dimensions of the cleft are given by its cross section (considered to be comparable with r_0) and its depth (r_d). Once the discharged proton diffuses out of the cleft, it is irreversibly dispersed in the bulk of the solution (Shimoni et al., 1993).

The reconstruction of the measured signal is a propagation of the proton, in space and time, along the whole length of the trajectory according to the transition probabilities. The propagation is carried out at successive time intervals and the probability density of the proton in calculated for each step along the pathway. The probability density inside the space enclosed within $r \le r_0$ is equated with the calculated fraction of the undissociated excited-pyranine molecule $\{\phi OH^*\}_t$. The product of $\{\phi OH^*\}_t$ times the radiative (plus nonradiative) decay of the excited molecule (τ = 4.8 ns), constitutes the predicted fluorescence decay as measured at 435 nm.

$$(I_{435})_t = [\{\phi OH^*\}_t \cdot \exp(-t/\tau)]$$

The fitting of the experimental signals was attained through an iterative search over the parameters' space, looking for a set that reproduced the experimental observations. Although a search in a five-dimensional space seems extremely laborious, it was facilitated by the fact that each parameter affects the dynamics in a very particular mode and within a limited time interval.

Fig. 6 depicts the effect of these parameters on the reaction kinetic, using a logarithmic Y scale. This presentation expands the later phase of the dynamics and allows evaluation of the contribution of each parameter during the full length of the observation time. In each frame the middle line corresponds with the best-fit values as listed in Table 1, while the other two were calculated with higher and lower values as detailed in the legend. For each frame only one parameter was varied, while all others are as listed in Table 1. In *A* the rate constant of the proton ejection from the pyranine molecule (κ_f) to the surrounding solvent was varied within the ~50% of the best-fit value. It can be seen that deviation of the lines from the experimental data is noticed right from t = 0 (please note that the time scale of *A* is only 6 ns). Actually, κ_f is the only term that controls the dynamics right from its most initial point. In the present case, any κ_f value that exceeds the range 0.65 ± 0.1 × 10^9 s^{-1} generates a systematic deviation that cannot be adjusted by modulation of all other parameters. The rate of recombination at the surface of the reaction sphere is given by κ_r. As discussed before (Gutman and Nachliel, 1997) this parameter is somewhat ambiguous and is not suitable for unique mechanistic interpretation. For this reason its value will not be discussed.

The other frames in Fig. 6 depict the effect of parameters characterizing the dispersion space. Frame *B* demonstrates the effect of the diffusion coefficient on the dynamics. The diffusion is expected to have a minor effect on the early phase of the reaction, while the probability density of the proton is still clustered near the pyranine anion. Indeed, we find that during the first 1–2 ns the diffusion coefficient has no effect on the ϕOH* decay curve. With the progression of time, as the proton probability density spreads over an increasing fraction of the diffusion space, the effect of D_{H+} on the reconstructed curves increases. A small diffusion coefficient implies that the proton will remain near the

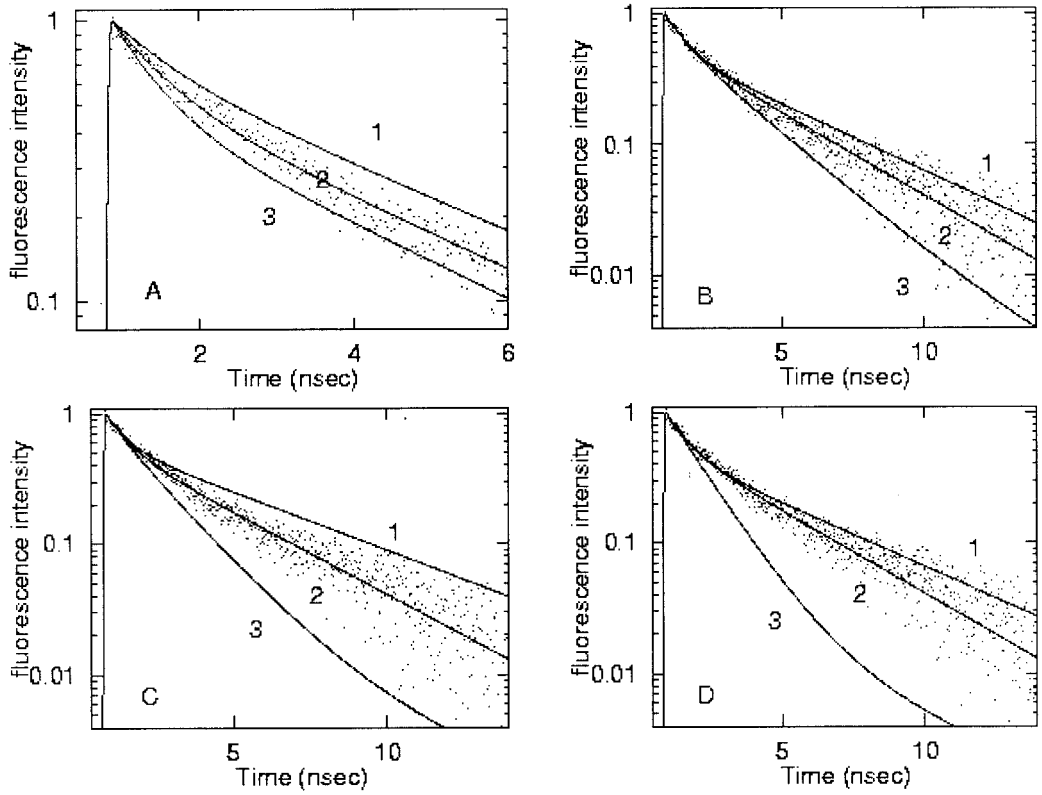

FIGURE 6 Evaluation of the accuracy of the simulating parameters. In each frame one of the parameters was varied and its effect on the dynamics was investigated. The range of variance is indicated below. The middle curve was calculated by the best-fit parameter as listed in Table 1. The ordinate is the fluorescence intensity normalized with respect to the maximal measured value. (*A*) The effect of κ_f on the reconstructed dynamics. Traces 1, 2, and 3 were calculated with $\kappa_f = 4$, 6.5, and 9×10^8 s^{-1}, respectively. Please note that the time scale of the frame is 6 ns. (*B*) The effect of the diffusion coefficient on the reconstruction dynamics. Traces 1, 2, and 3 were calculated with $D_{H+} = 1$, 3, and 9×10^{-5} cm^2 s^{-1}, respectively. (*C*) The effect of the electrostatic force, given by the Debye radius. Traces 1, 2, and 3 were calculated with $R_D = 80$, 50, and 28.3 Å, respectively. (*D*) The effect of the length of the binding cavity on the dynamics. Traces 1, 2, and 3 were calculated with $r_d = 25$, 17, and 9 Å, respectively.

pyranine anion with a subsequent increase in recombination probability, and a larger fraction of the ϕOH* population would decay by the relatively slower radiative pathway. Fast diffusion would let the proton escape from the cleft and the fast dissociation of ϕOH* would dominate fluorescence dynamics. The lower curve in *B* was calculated with the normal value of the diffusion coefficient of proton in bulk water (9×10^{-5} cm^2 s^{-1}), while the upper one corresponds with only 10% of this value. Reconstruction carried out with $D_{H+} = 3 \pm 1 \times 10^{-5}$ cm^2 s^{-1} exhibited no systematic deviations from the measured transient.

Frame *C* depicts the effect of the intensity of the electrostatic forces expressed by the Debye radius (see Eq. 2). Strong electrostatic attraction between the reactants (large R_D) implies that the proton will remain in the vicinity of the pyranine anion for a long time, and recombination that regenerates ϕOH* will be a frequent event. In such a scenario the decay of ϕOH* emission will be slow (*lower curve*). A weak electrostatic interaction will reverse the situation and the ϕOH* population will vanish rapidly. The shape of the curves, calculated with varying intensity of the electrostatic potentials, exhibits "spreading" from a common time point earlier than in *B*. The best-fit curve has a value of ~50 ± 10 Å, indicating that the electrostatic attraction of the bound dye extends beyond the dimension of the cavity where it is located. Such an extension of the electrostatic field suggests that a low dielectric constant matrix surrounds the space where the dye is bound.

In *D* we investigated to what extent the geometry of the reaction space affects the reconstructed dynamics. The calculations were carried out for a cylindrical cavity having a radius comparable to that of the pyranine anion and a depth of 9 Å (*upper curve*) or 25 Å (*bottom curve*). In a deep cavity, the proton will remain for a long time under the influence of the intensified electrostatic attraction so that the probability density of protons in the cleft is prolonged with subsequent slower relaxation of the ϕOH* population. According to the shape of the curve we estimate the depth of the cleft to be between 9 and 17 Å. The shape of the curves calculated with varying depths of cavity exhibit a special feature not observed in the other frames; the time point at which the lines are "spreading" varies with the depth of the

cavity. Thus, each of the parameters leaves a distinct mark on the shape of the relaxation curve, a feature that assists in the fitting of the parameters to the measured curve.

During the reconstruction of proton dissociation in other proteins such as apomyoglobin (Shimoni et al., 1993) or the PhoE channel (Gutman et al., 1992b) an additional parameter had to be incorporated in the reconstruction: the reaction of the discharged proton with the carboxylates lining the cavity. In the reconstruction of lac permease we found no evidence for that reaction. Moreover, inclusion of an intracavity proton-carboxylate reaction distorted the dynamics to a point where no combination of the other parameters could make them fit the experiments.

Quantitative evaluation of the parameters

The adjustable parameters reproducing the measured dynamics are listed in Table 1. The first parameter, κ_f, is the rate constant of proton dissociation from the excited pyranine molecule and controls the most initial phase of the decay. This parameter can be easily measured with an accuracy of $\pm 5\%$. The modulation of this rate by the environment can be used for quantitating the activity of the water at the first solvation shell of the excited molecule (Table 1, row 2) (Huppert et al., 1982). The rates measured for the lac permease-bound pyranine are much slower than in bulk water, indicating that the water molecules in the cavity strongly interact with the protein. The ordering of the solvent molecules by the protein retards their capacity to rotate and solvate the discharged proton at a rate that is competitive with the proton's tendency to recombine with the excited anion. The activity of the water as estimated by the rate of dissociation is rather low ($a_{(water)} = 0.71$), and comparable with the activity measured for the heme-binding site of the apomyoglobin, where the pyranine almost fills the whole intraprotein cavity (Shimoni et al., 1993). After the addition of saturating concentrations of lactose, κ_f was increased by 25%. This effect is not to be confused with a general feature of concentrated solution of sugars (over 1 M) where enhancement of the protein's solvation shell was reported (Timasheff, 1992; Arakawa, 1982). For this reason we consider the effect to be a specific one, resulting from the interaction of the substrate with its native binding site. Although the acceleration of κ_f is experimentally significant, because of the logarithmic correlation between rates of dissociation and the a_{water} (Huppert et al., 1982; Gutman et al., 1982; Gutman and Nachliel, 1990), the calculated increment of water activity is rather small. Both lactose and the TDG used in the steady-state fluorescence measurements failed to eject the pyranine from the binding cleft, suggesting that the dye is not located within the space where the substrate is bound. However, the two domains are not isolated and binding of the substrate affects the environment of the dye. The lac permease is sufficiently flexible and dynamic in nature (Patzlaff et al., 1998; Johnson and Brooker, 1999) so that the scissors motion of the helices, induced by the substrate (Wu et al., 1999), propagates the perturbation to other sites of the protein.

The diffusion coefficient (D_{H+}) of the proton in the cavity is ~30% of its diffusivity in bulk water. Considering that the diffusion of proton in water proceeds by the Grotthuss mechanism, which is sensitive to the rate of random rotation of the water molecules (Agmon, 1999), the reduced diffusion coefficient is in accord with the lower activity of the water in the site. We wish to point out that although the estimation of $a_{(water)}$ on the basis of κ_f mostly reflects the water molecules next to the dye, the measured diffusion coefficient suggests that most, or all, of the water in the cleft is effectively immobilized by the protein.

The electrostatic potential in the binding site was derived according to Eq. 2 using the value of R_D as needed to reconstruct the measured signals. In comparison with the standard value for pyranine anion in water, $R_D = 28.3$ Å (25°C), the values determined for the pyranine binding site and in the presence of lactose were 50 Å and 42 Å, respectively. Both values correspond with an environment that amplifies the electrostatic potential within the cleft, and expands the region of influence of a charge beyond the limits measured in water. Reflection of similar properties to the substrate-binding site suggests that the enhancement of the charge-dipole attractions tighten the interactions between the substrate and the protein. Addition of lactose reduced the pyranine's apparent R_D value beyond the limits of experimental error. Thus, the conformation change imposed by the binding of lactose modulated the electrostatic potential within the pyranine-binding site in a mode corresponding with better screening of the anion's charge. Combining this effect with the acceleration of the dissociation reaction, we suggest that the binding of the substrate enhanced the solvation of the pyranine-binding cleft.

CONCLUDING REMARKS

In this study we present evidence for the binding of pyranine to lac permease at a site that differs from the substrate-binding site, yet the two can interact with one another through the flexible matrix of the protein. In the bound state, the pyranine exhibits physical and chemical properties that differ from those of the dye in bulk water. The analysis of the fluorescence decay signals indicates that the pyranine-binding site is a cleft (some 9 to 17 Å deep), where at least a single positive charge is present. Water molecules, which strongly interact with the protein's side chains, fill the intracavity space. As a result, the diffusion coefficient of the proton, the chemical potential of the water, and the effective dielectric constant generate a local environment that differs from the bulk. In such a space the enhancement of the electrostatic potential affects polar molecules through charge-dipole or dipole-dipole interactions, and the reduction of the activity of the water suppresses the dissociation

of acidic residues. These properties, if attributed to the substrate conducting pathway, may explain some of the forces operating on the substrate in the cavity. The reduced activity of the water strips the substrate from some of its solvating water molecules and replaces them by direct interaction with the protein. In parallel, the lower dielectric constant enhances the binding of the proton to the protein, thus keeping a tight seal that prevents protons from leaking though the enzyme.

The lac permease is a flexible protein that assumes more than one conformation. The transition between the states is associated with the catalytic cycle. Both protonation of the protein and the binding of substrate shift the dominant conformation of the enzyme. The present study demonstrated that lac permease could react with pyranine, by a combination of electrostatic and hydrophobic interactions, to form a complex where the dye is inserted into a rather deep cleft in the protein. Furthermore, the dye's binding site is not in the substrate-conducting cavity, as the addition of lactose (but not sucrose) modifies the site without expelling the dye. We suggest that the inter-helix, scissor-like motion imposed by the substrate binding (Wu et al., 1999) causes the pyranine site to be better solvated.

The authors are grateful to Johannes Le-Coutre for his generous provision of the enzyme and to Ronald H. Kaback for his interest and criticism.

This research was supported by the United State-Israel Bi-National Science Foundation (B.S.F., Grant 97-130) and the German-Israeli Foundation for Scientific Research and Development (G.I.F., Grant I-140-207.98).

REFERENCES

Agmon, N. 1999. Proton solvation and proton mobility. *Israel J. Chem.* 39:493–502.

Agmon, N., E. Pines, and D. Huppert. 1988. Geminate recombination in proton-transfer reaction. II. Comparison of diffusional and kinetic schemes. *J. Chem. Phys.* 88:5631–5638.

Agmon, N., and A. Szabo. 1990. Theory of reversible diffusion-influenced reaction. *J. Chem. Phys.* 92:5270–5284.

Arakawa, T. T. S. 1982. Stabilization of protein structure by sugars. *Biochemistry.* 21:6536–6544.

Clement, N. R., and J. M. Gould. 1981. Pyranine as a probe of internal aqueous proton concentration in phospholipid vesicles. *Biochemistry.* 20:1534–1538.

Forster Th., and A. Volkers. 1975. Kinetics of proton transfer reactions involving hydroxypyrene-trisulfonate in aqueous solution by nanosecond laser absorption spectroscopy. *Chem. Phys. Lett.* 34:1–5.

Frillingos, S., M. Sahin-Toth, J. Wu, and H. R. Kaback. 1998. Cys-scanning mutagenesis: a novel approach to structure-function relationship in polytopic membrane proteins. *FASEB J.* 12:1281–1299.

Gutman, M., D. Huppert, and E. Nachliel. 1982. Kinetic studies of proton transfer in the microenvironment of a binding site. *Eur. J. Biochem.* 121:637–642.

Gutman, M., and E. Nachliel. 1990. The dynamic aspects of proton transfer processes. *Biochim. Biophys. Acta.* 1015:391–414.

Gutman, M., and E. Nachliel. 1993. Study of the semi ordered water in an active site by time resolved measurement of a single diffusing proton. *Solid State Ionics.* 61:229–234.

Gutman, M., and E. Nachliel. 1997. Time-resolved dynamics of proton transfer in proteinous systems. *Annu. Rev. Phys. Chem.* 48:329–356.

Gutman, M., E. Nachliel, and S. Kiryati. 1992a. Dynamic studies of proton diffusion in mesoscopic heterogeneous matrix, the interbilayer space between phospholipids membranes. *Biophys. J.* 63:281–290.

Gutman, M., Y. Tsfadia, A. Masad, and E. Nachliel. 1992b. Quantitation of physical-chemical properties of the aqueous phase inside the PhoE ionic channel. *Biochim. Biophys. Acta.* 1109:141–148.

Huppert, D., E. Kolodney, M. Gutman, and E. Nachliel. 1982. Effect of water activity on the rate of proton dissociation. *J. Am. Chem. Soc.* 104:6949–6953.

Huppert, D., E. Pines, and N. Agmon. 1990. Long-time behavior of reversible geminate recombination reactions. *J. Otc. Soc. Am.* 7:1545–1550.

Jessen-Marshall, A. E., N. J. Parker, and R. J. Brooker. 1997. Suppressor analysis of mutations in the loop 2–3 motif of lactose permease: Evidence that glycine-64 is an important residue for conformational changes. *J. Bacteriol.* 179:2616–2622.

Johnson, J. L., and R. J. Brooker. 1999. A K319N/E325Q double mutant of the lactose permease cotransports H+ with lactose. Implications for a proposed mechanism of H+/lactose symport. *J. Biol. Chem.* 274: 4074–4081.

Kaback, H. R. 1997. A molecular mechanism for energy coupling in a membrane transport protein, the lactose permease of *Escherichia coli. Proc. Natl. Acad. Sci. U.S.A.* 94:5539–5543.

Kaback, H. R., J. Voss, and J. Wu. 1997. Helix packing in polytopic membrane proteins: the lactose permease of *Escherichia coli*. *Curr. Opin. Struct. Biol.* 7:537–542.

Kaback, H. R., and J. Wu. 1997. From membrane to molecule to the third amino acid from the left with a membrane transport protein. *Q. Rev. Biophys.* 30:333–364.

Krissinel, E. B., and N. Agmon. 1996. Spherical symmetry diffusion problem. *J. Comp. Chem.* 17:1085–1098.

Patzlaff, J. S., J. A. Moeller, B. A. Barry, and R. J. Brooker. 1998. Fourier transform infrared analysis of purified lactose permease: a monodisperse lactose permease preparation is stably folded, alpha-helical, and highly accessible to deuterium exchange. *Biochemistry.* 37:15363–15375.

Pazdernik, N. J., S. M. Cain, and R. J. Brooker. 1997. An analysis of suppressor mutations suggests that the two halves of the lactose permease function in a symmetrical manner. *J. Biol. Chem.* 272: 26110–26116.

Pines, E., D. Huppert, and N. Agmon. 1988. Geminate recombination in excited-state proton transfer reaction: numerical solution of the Debye-Smoluchowski equation with back reaction and comparison with experimental results. *J. Chem. Phys.* 88:5620–5630.

Rochel, S., E. Nachliel, D. Huppert, and M. Gutman. 1990. Proton dissociation dynamics in the aqueous layer of multilamellar phospholipid vesicles. *J. Membr. Biol.* 118:225–232.

Shimoni, E., Y. Tsfadia, E. Nachliel, and M. Gutman. 1993. Gaugement of the inner space of the apomyoglobin's heme binding site by a single free diffusing proton. I. Proton in the cavity. *Biophys. J.* 64:472–479.

Timasheff, S. N. 1992. Water as ligand: preferential binding and exclusion of denaturants in protein unfolding. *Biochemistry.* 31:9857–9865.

Viitanen, P., M. J. Newman, D. L. Foster, T. H. Wilson, and H. R. Kaback. 1986. Purification, reconstitution, and characterization of the lac permease of *Escherichia coli*. *Methods Enzymol.* 125:429–452.

Weller, A. 1961. Excited state proton transfer. *Prog. Reaction Kinetic.* 1:198–214.

Wu, J., D. Hardy, and H. R. Kaback. 1999. Site-directed chemical cross-linking demonstrates that helix IV is close to helices VII and XI in the lactose permease. *Biochemistry.* 38:1715–1720.

Wu, J., D. M. Perrin, D. S. Sigman, and H. R. Kaback. 1995. Helix packing of lactose permease in *Escherichia coli* studied by site-directed chemical cleavage. *Proc. Natl. Acad. Sci. USA.* 92:9186–9190.

Yam, R., E. Nachliel, S. Kiryati, M. Gutman, and D. Huppert. 1991. Proton transfer dynamics in the nonhomogeneous electric field of a protein. *Biophys. J.* 59:4–11.